Supporting information

Immune Checkpoint Inhibition in GBM Primed with Radiation by Engineered Extracellular Vesicles

Tian Tian,[†,§,#,*] Ruyu Liang,[§,#] Gulsah Erel-Akbaba,[†,‖] Lorenzo Saad,[†] Pierre J. Obeid,[⊥] Jun Gao,[§,*] E. Antonio Chiocca,[¶] Ralph Weissleder,[▽] and Bakhos A. Tannous[†,*]

[†]Experimental Therapeutics and Molecular Imaging Unit, Department of Neurology, Neuro-Oncology Division, and [▽]Center for Systems Biology, Massachusetts General Hospital, Harvard Medical School, Boston, Massachusetts 02129, United States

[§]Department of Neurobiology, Key Laboratory of Human Functional Genomics of Jiangsu, Nanjing Medical University, Nanjing, Jiangsu 211166, China

[‖]Department of Pharmaceutical Biotechnology, Faculty of Pharmacy, Izmir Katip Celebi University, Izmir 35620, Turkey

[⊥]Department of Chemistry, University of Balamand, Al Kurah, Deir El-Balamand, P.O. Box 100, Tripoli, Lebanon

[¶]Department of Neurosurgery, Brigham and Women's Hospital, Harvard Medical School, Boston, Massachusetts 02115, United States

[#]These authors contributed equally to this work.

*Corresponding authors:

Bakhos A. Tannous, Ph.D.

E-mail: btannous@hms.harvard.edu.

Tian Tian, Ph.D.

E-mail: ttian@njmu.edu.cn.

Jun Gao, Ph.D.

E-mail: gaojun@njmu.edu.cn.

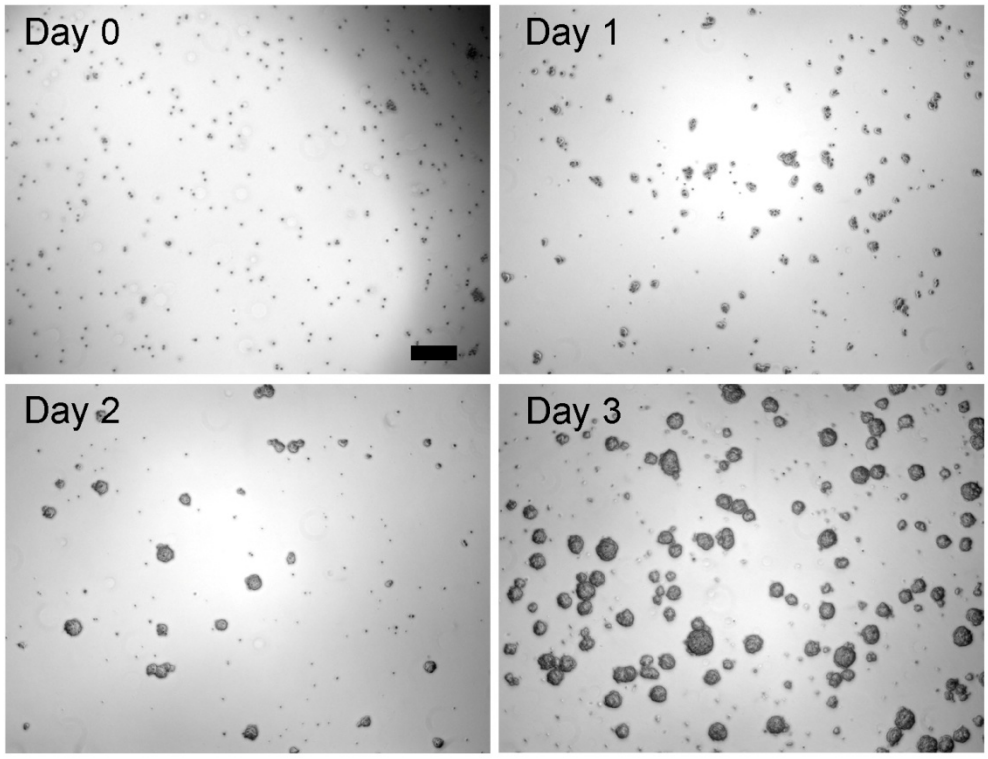

Figure S1. Bright-field images of ReN cells cultured for 3 days; scale bar, 200 μm.

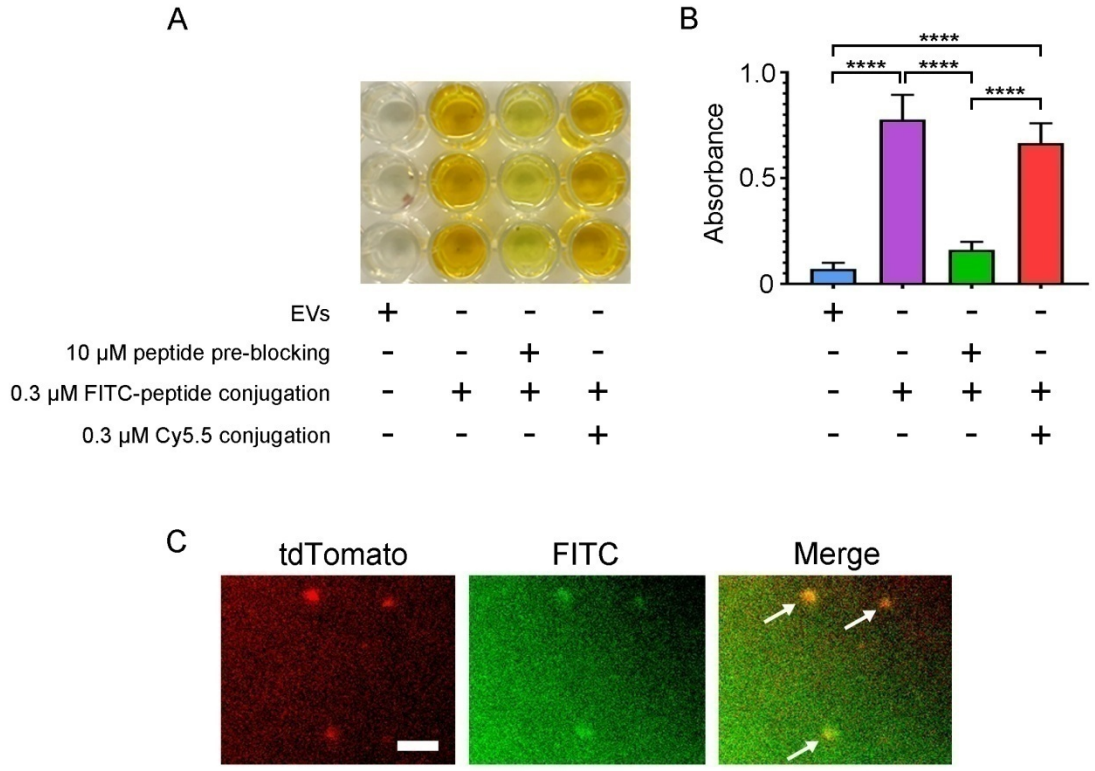

Figure S2. Confirmation of c(RKDyK) peptide on EV surface. DBCO groups were introduced to EV surface and reacted with azide-functionalized peptide and azide-FITC or control. Non-labeled c(RKGyK) peptide was used to block DBCO on EVs by a 12-h pre-incubation. (A) Representative image of ELISA microplate developed with tetramethylbenzidine. (B) ELISA absorbance of FITC on EVs. Data are presented as mean ±SEM (n = 6); ****P < 0.0001 by One-way ANOVA. (C) Fluorescence images of tdTomato-labeled EVs after conjugation of FITC-labeled c(RKDyK) peptide. Red shows tdTomato, green is FITC. Arrows indicate the co-localization between tdTomato and FITC on EVs; scale bar, 1 μm.

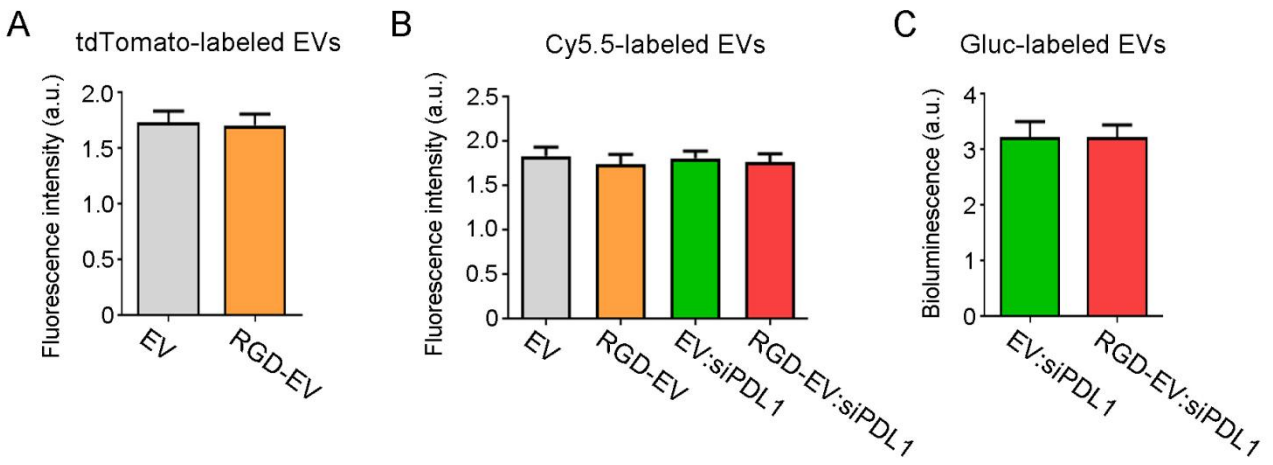

Figure S3. Labeling efficiency of EVs with different optical reporters. (A,B) Fluorescence intensities of 10 μg tdTomato- or Cy5.5-labeled EVs (solubilized with 0.5% Triton X-100 in 100 μL PBS). (C) Bioluminescence levels of 10 μg Gluc-labeled EVs (in 50 μL PBS). Data presented as mean ±SEM (n = 6); No statistical differences were observed between different groups by student's *t*-test or One-way ANOVA.

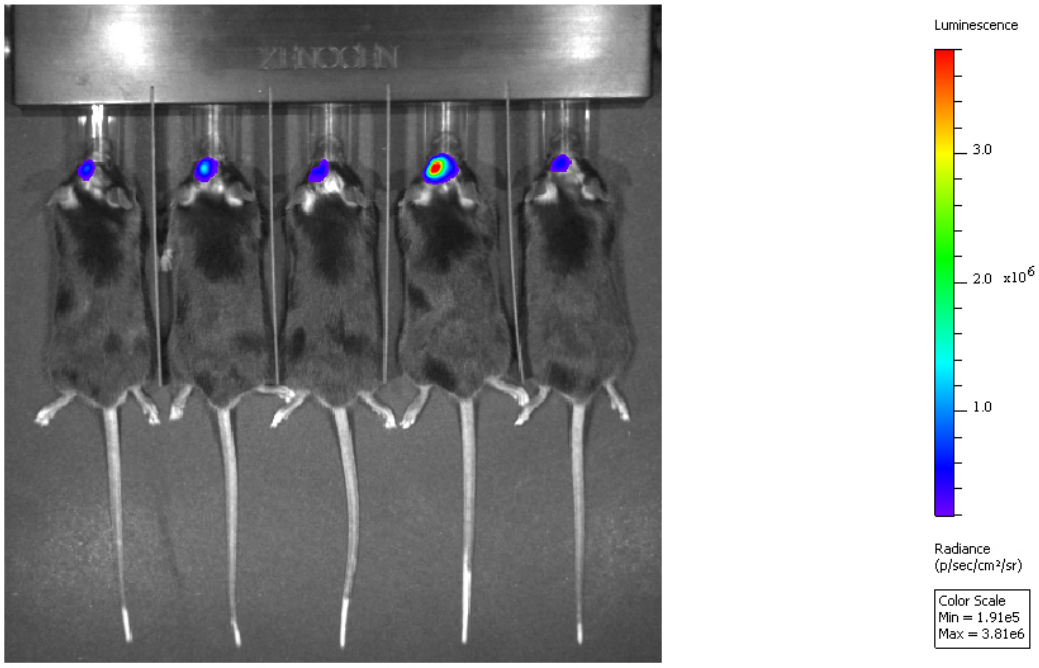

Figure S4. Fluc bioluminescence images confirming tumor formation on day 7 post-implantation of GL261 cells.

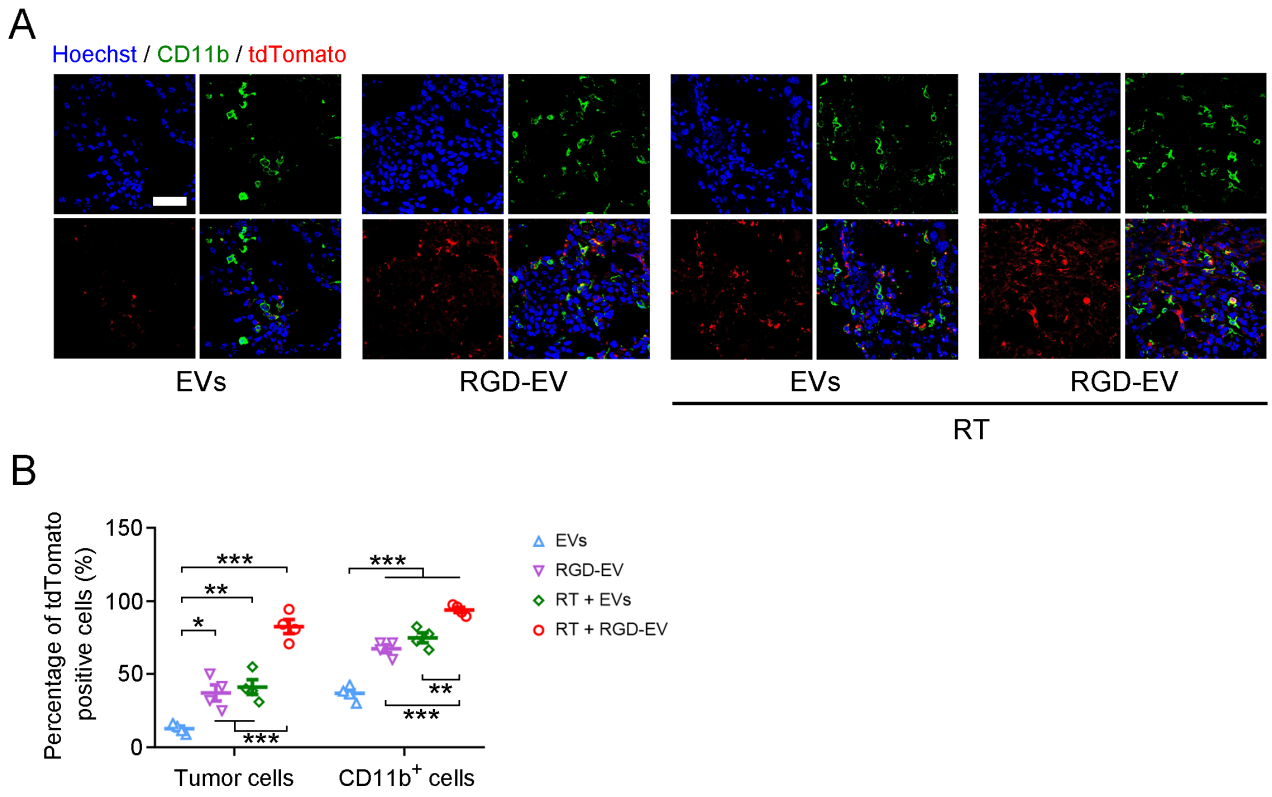

Figure S5. Effect of RT on EV uptake by tumor and microenvironment. (A) GBM-bearing mice were irradiated and injected with tdTomato-labeled EVs or RGD-EVs. Representative fluorescence images of EVs (red) in $CD11b^+$ cells (GFP) 6 h post-EVs administration; blue indicates nuclei; scale bar, 50 μm. (B) Statistical percentages of tdTomato-positive tumor cells (representative fluorescence images are shown in Figure 2D) and $CD11b^+$ cells. Data presented as mean ±SEM (n = 4); *P < 0.05, **P < 0.01, ***P < 0.001 by One-way ANOVA.

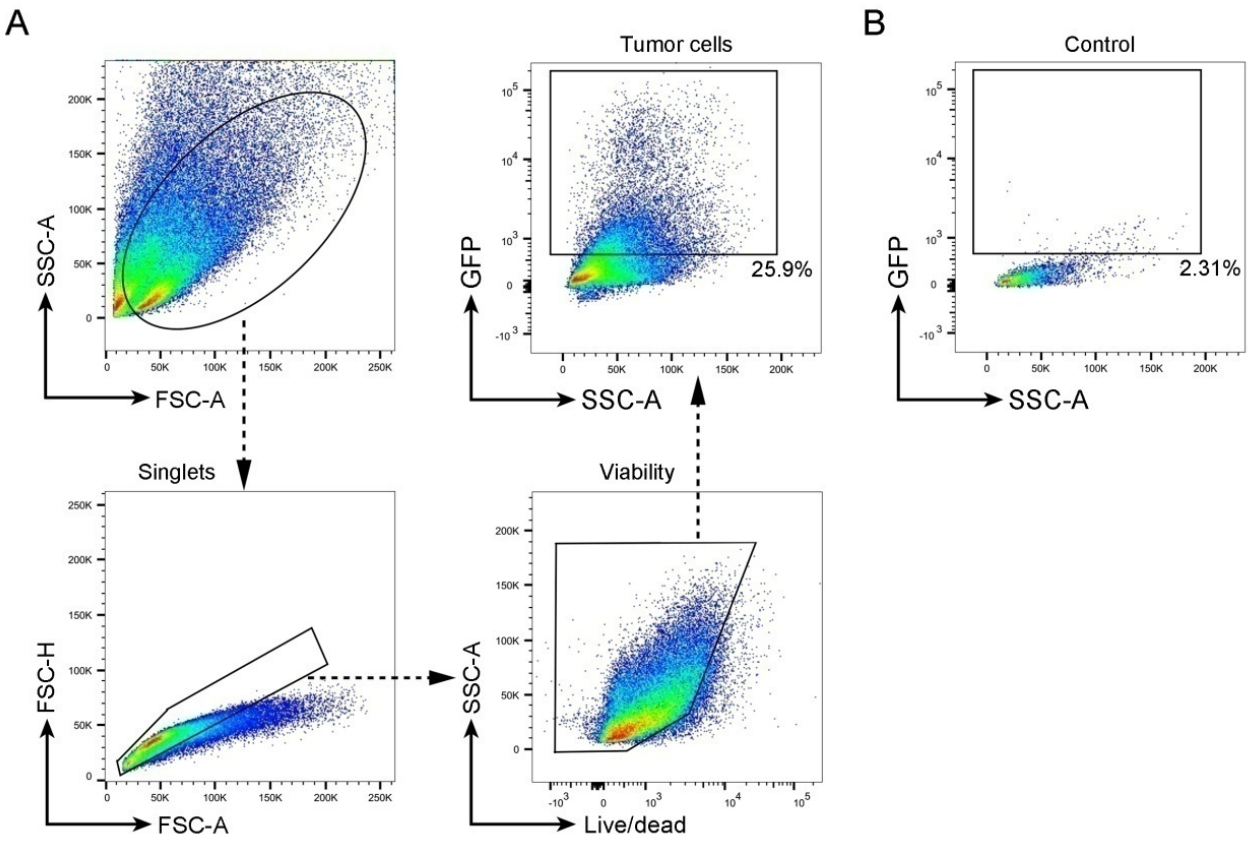

Figure S6. (A) Sorting strategy for GFP-expressed tumor cells in the GL261-GFP syngeneic mouse GBM model using flow cytometry. (B) Samples from the GFP-negative GL261 glioma model as a negative control.

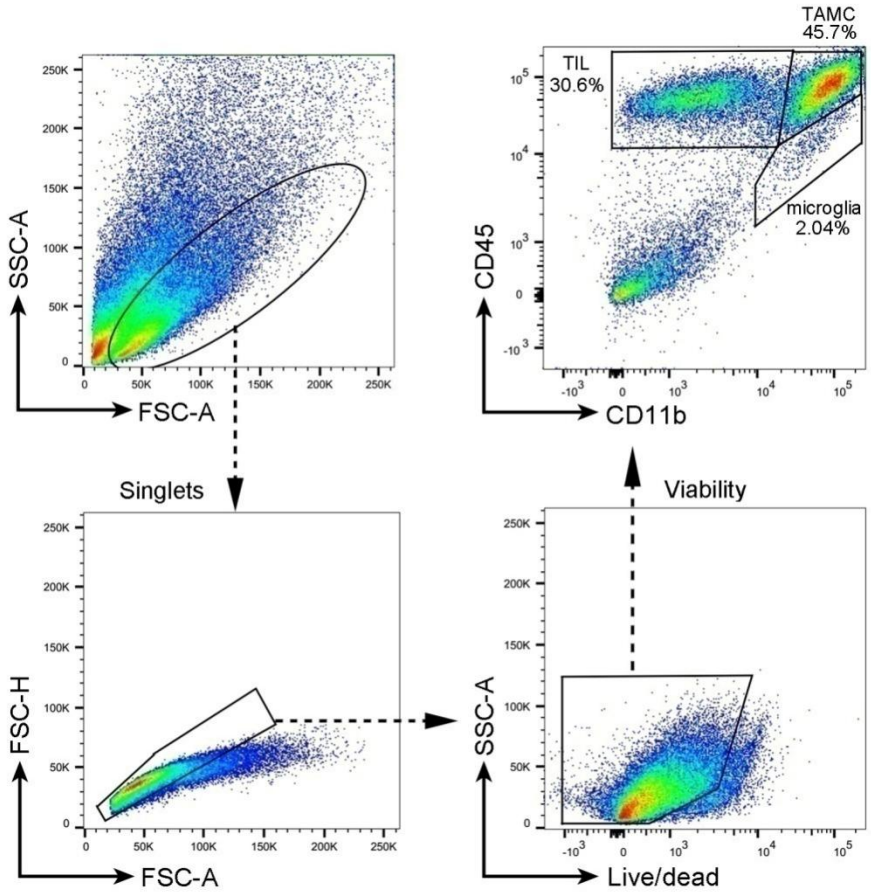

Figure S7. Phenotyping of immune cells (TAMCs, TILs, and microglia) in the GL261 syngeneic mouse GBM model by flow cytometry analysis.

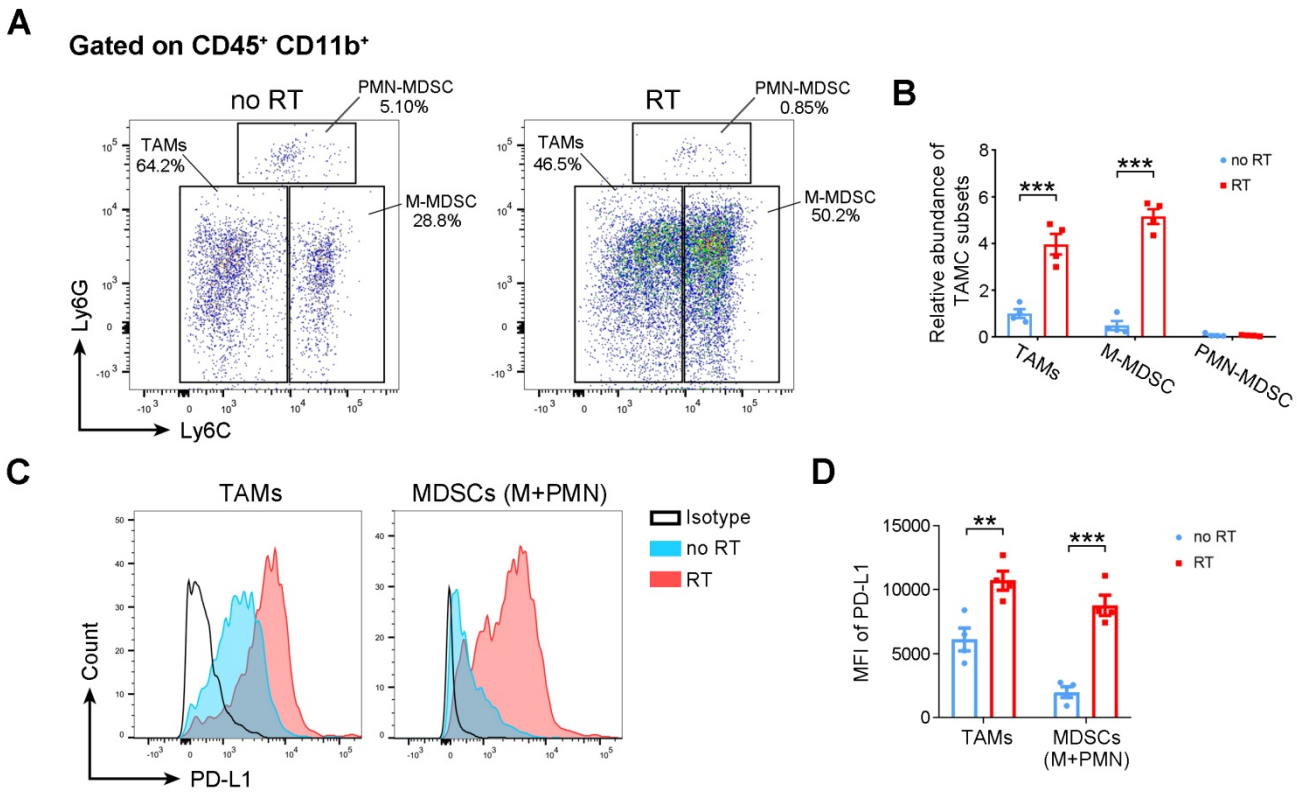

Figure S8. Flow cytometric analysis of TAMC subsets in GBM post-RT. (A) Gating strategy for TAMC subsets [TAMs, monocytic MDSCs (M-MDSC), polymorphonuclear MDSCs (PMN-MDSC)] and their representative percentages in TAMCs. (B) Abundance of TAMC subsets determined as percentages in Ly6C-Ly6G plots multiplied by the percentages of TAMCs in CD45-CD11b plots, and normalized to TAMs without RT group. Representative histograms (C) and MFI (D) of PD-L1 in TAMs and MDSCs (given that PMN-MDSC portion was very few, M-MDSC and PMN-MDSC were analyzed together). Data are presented as mean ±SEM (n = 4); **P < 0.01, ***P < 0.001 by student's *t*-test.

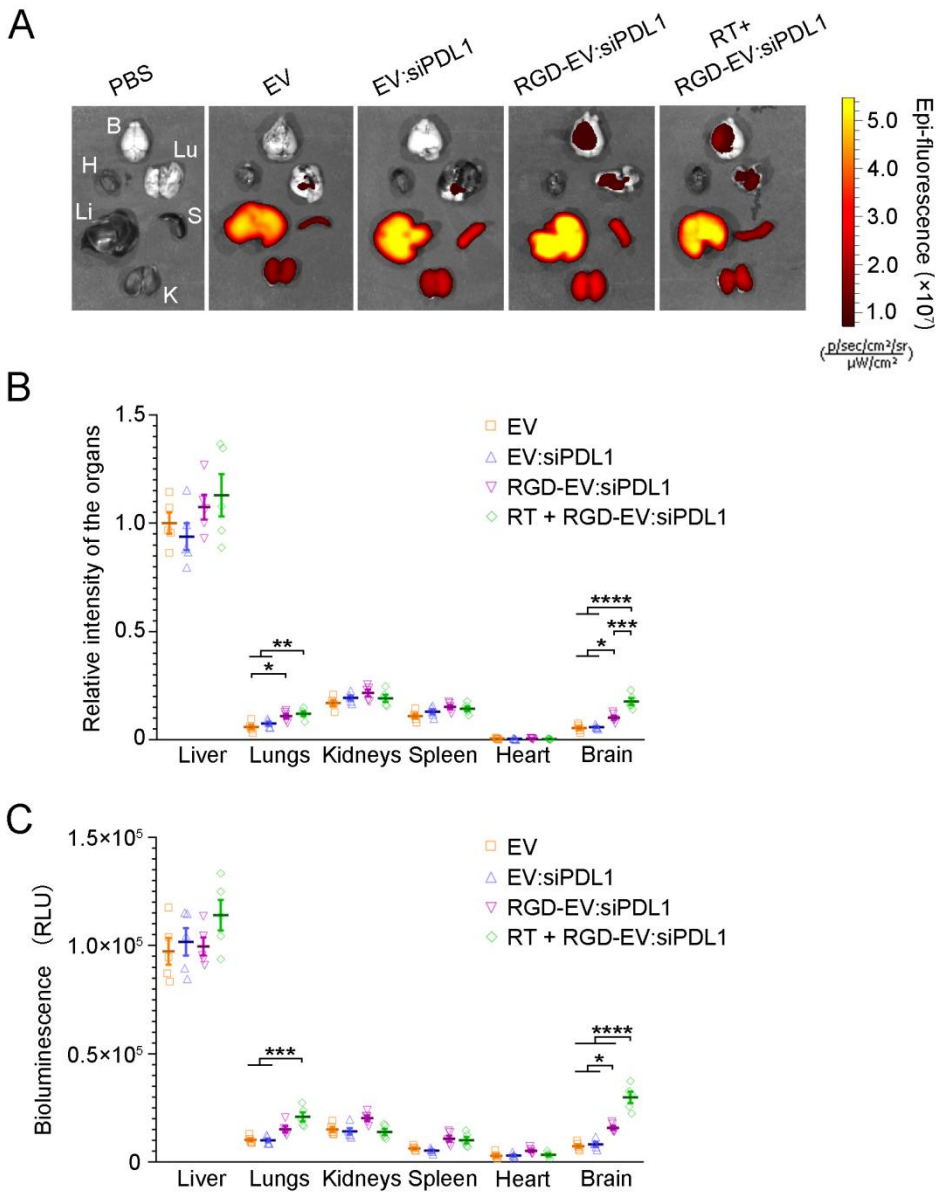

Figure S9. Biodistribution of engineered EVs analyzed by NIRF imaging and bioluminescence. (A) Mice-bearing tumors primed with 5-Gy RT were injected with Cy5.5-labeled EVs or EV:siPDL1 or RGD-EV:siPDL1. Twenty-four hours later, different organs were removed and analyzed by NIRF imaging; B, brain; H, heart; Lu, lungs; Li, liver; S, spleen; K, kidneys. (B) Quantification of fluorescence intensities in different organs. (C) Mice-bearing tumors primed with 5-Gy RT were injected with Gluc-labeled EV or EV:siPDL1 or RGD-EV:siPDL1. Gluc activity was measured in different organs collected from mice following transcardial perfusion with PBS. Data presented as mean ±SEM (n = 5); *P < 0.05, **P < 0.01, ***P < 0.001, ****P < 0.0001 by One-way ANOVA.

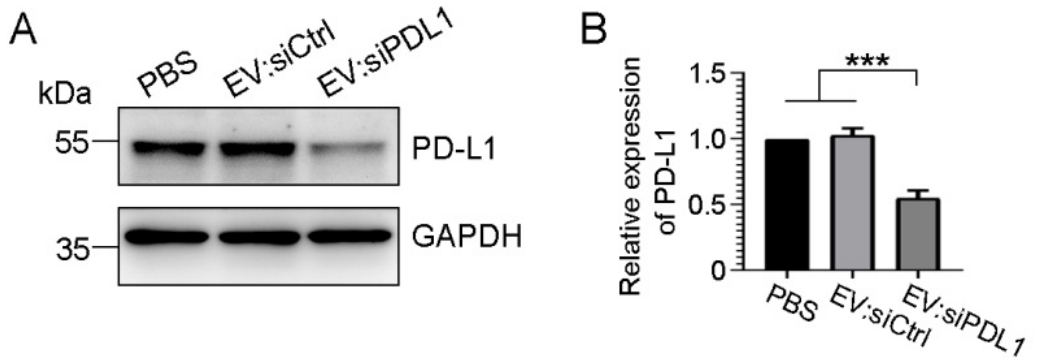

Figure S10. PD-L1 knockdown in GL261 cells. GL261 cells were treated with PBS or 10 μg of either EV:siCtrl or EV:siPDL1. (A) Forty-eight hours later, cell lysates were analyzed by Western blotting using PD-L1 and GAPDH as a loading control. (B) Relative PD-L1 levels analyzed by densitometry. Data presented as mean ±SEM (n = 4); ***P < 0.001 by One-way ANOVA.

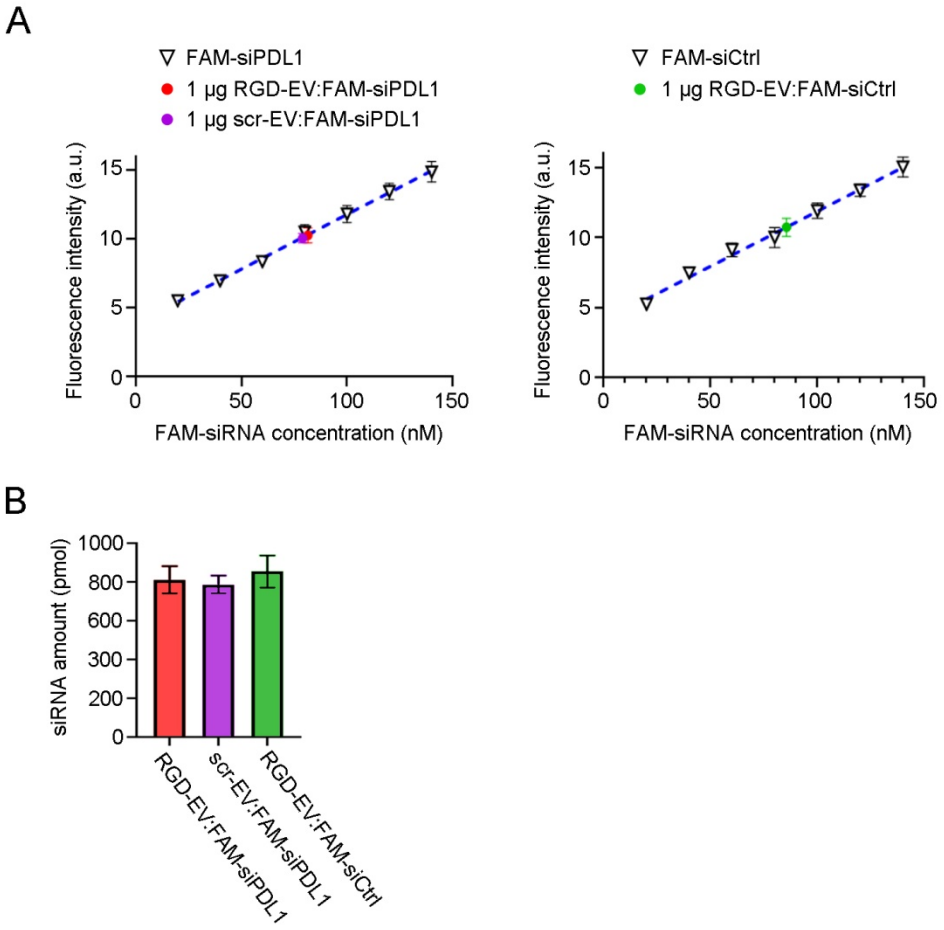

Figure S11. Estimation of siRNA amount incorporated onto EVs. (A,B) Black triangles show fluorescence intensities of synthesized FAM-conjugated siRNAs at 20-140 nM. Blue dashed lines represent standard curves by linear fitting. The average fluorescent intensities of 1 μg RGD-EV:FAM-siPDL1, scr-EV:FAM-siPDL1, or RGD-EV:FAM-siCtrl (solubilized by 0.5% Triton X-100 in 100 μL PBS) are indicated by red, purple, or green dot, respectively. The corresponding concentrations of incorporated siRNAs are calculated according to each standard curve. (B) Estimation of siRNA amount incorporated onto EVs with 100 μg total protein. Data presented as mean ±SEM (n = 4); No statistical differences were observed between different groups as analyzed by One-way ANOVA.

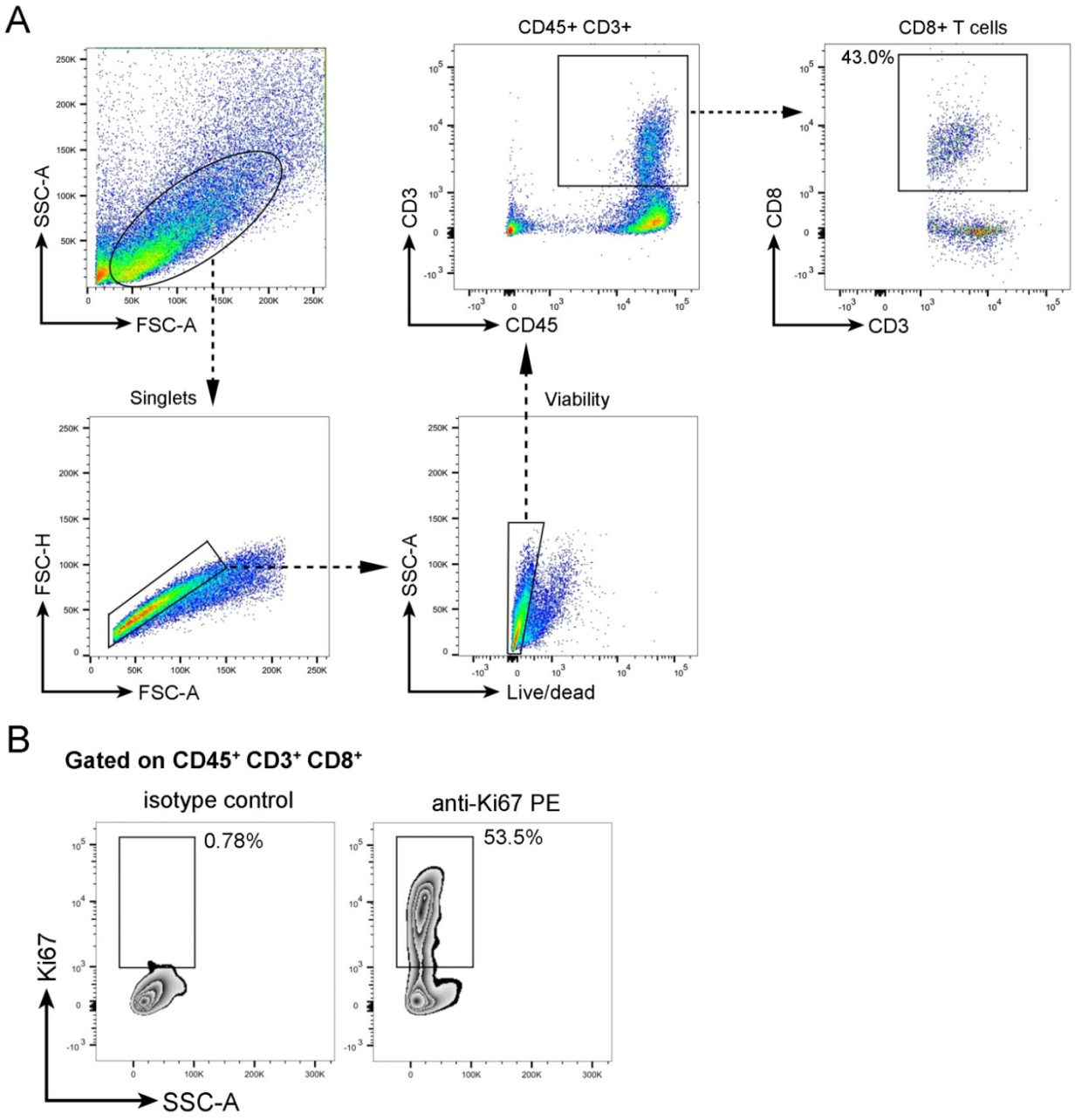

Figure S12. (A) Sorting strategy for $CD8^+$ T cells in the GL261-GFP syngeneic mouse GBM model by flow cytometry. (B) Analysis of Ki67 expression in $CD8^+$ T cells.

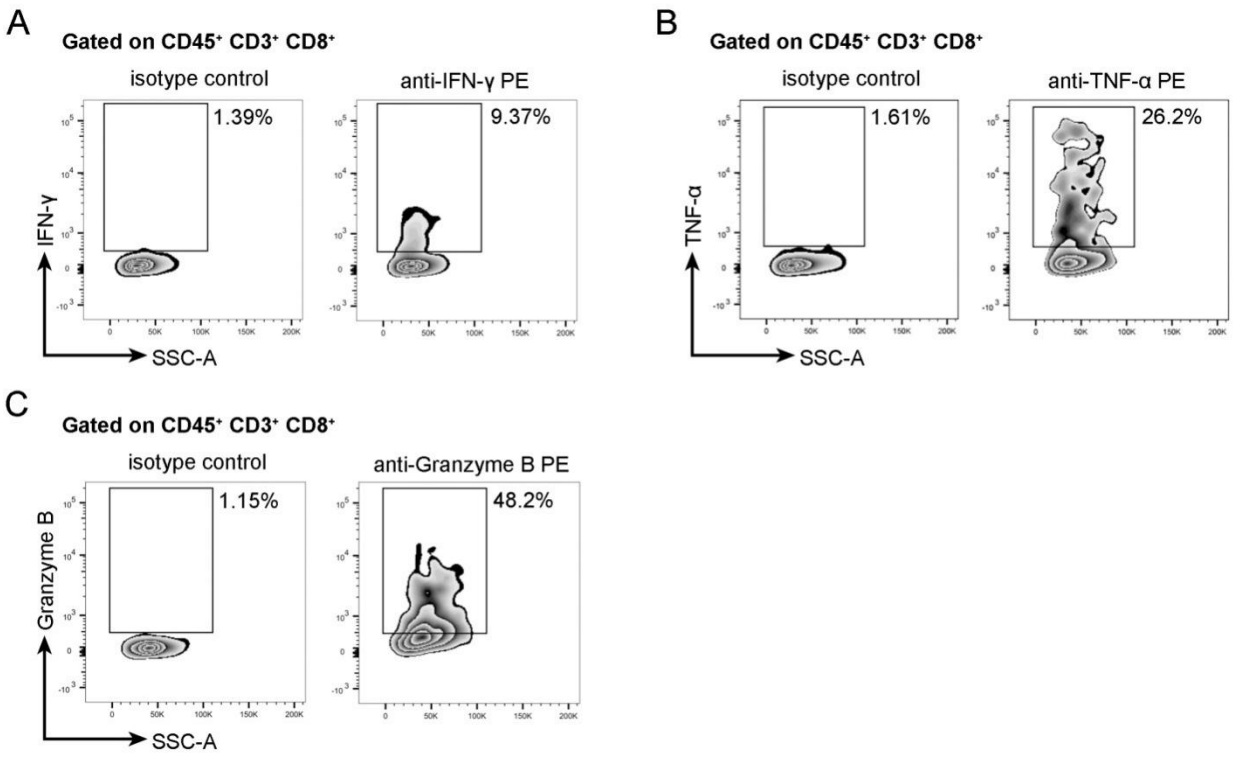

Figure S13. Flow cytometric analysis of (A) IFN-γ, (B) TNF-α, and (C) Granzyme B expression in $CD8^+$ T cells from mouse GBM model.